

Crystal-to-glass-transition induced elastic anomaly of cerium-iron multilayer films and texture-related mechanical properties after hydrogenation

R. Hassdorf, M. Arend, and W. Felsch

I. Physikalisches Institut, Universität Göttingen, Bunsenstrasse 9, D-37073 Göttingen, Germany

(Received 21 November 1994)

The flexural modulus E_F of pure and hydrided cerium-iron multilayer films has been measured at 300 K as a function of the modulation wavelength Λ using a vibrating-reed technique. E_F is strongly correlated to the structure of the layered systems. In the pure Ce/Fe multilayers, the Fe sublayers show a structural transition from an amorphous to the bcc crystalline phase for a thickness near 20 Å. At this transition, the modulus E_F is reduced by $\sim 70\%$. The elastic softening occurs already, as a precursor to the structural change, for the crystalline Fe sublayers somewhat above the thickness for amorphous growth. This behavior reveals close similarities to the crystal-to-glass transition in bulk metallic alloys and compounds which seems to be driven by a shear instability of the crystal lattice. Hydrogenation leads to multilayers built of CeH_{1.2}/Fe. The Fe sublayers grow in the bcc structure above 10 Å, with a pronounced (110) or (111) texture for low- or room-temperature deposition. The flexural moduli are larger as compared to the nonhydrided multilayers and distinctly different for the two Fe textures. A simple calculation shows that the texture-related differences mainly result from the bulk properties of the Fe layers, but a contribution of interfacial effects cannot be excluded.

I. INTRODUCTION

The variety of anomalies in the elastic properties of artificial metallic multilayers and superlattices and their relation to interface effects have received great attention in the last decade. Drastically reduced shear moduli and significantly enhanced Young's and biaxial moduli have been observed when the periodicity length of the modulated structure was reduced to about 20 Å, sometimes in the same system.¹ It is generally accepted that these elastic anomalies (often referred to as "supermodulus effects") are correlated with structural changes resulting from interface effects, but the exact nature of this interplay is not well understood at present. Theoretical models proposed involve changes in the electronic structure associated with the additional periodicity of the superlattice,² charge transfer,³ or strain accumulation at the interfaces.⁴

In view of the close correlation between the structural and elastic properties in such layered metallic systems it is particularly interesting to study the elastic response of a multilayer as one of the constituent materials undergoes a structural transition. For instance, in Fe/Cu superlattices the fcc-bcc structural phase transition in the Fe layers occurring at a certain Fe and Cu layer thickness is signaled by a clear-cut minimum in the surface phonon wave velocity;⁵ in W/Ni multilayers this quantity gradually decreases with decreasing bilayer repeat length down to a critical thickness where both layers transform into an amorphous structure.⁶

In this paper we present a characterization of the elastic properties of Ce/Fe multilayers determined by a vibrating-reed technique. The layers combine, in a periodic stack, a soft (Ce) with a stiff (Fe) component, which both grow in an amorphous structure below and in a crystalline structure above a critical thickness, which is

near 20 Å for Fe and near 60 Å for Ce. These multilayers can be prepared with sharp interfaces⁷ and have been thoroughly characterized previously by different techniques.⁸⁻¹⁰ The absence of crystalline long-range order in the amorphous phase of the Fe layers has a drastic bearing on the magnetic properties of the multilayers. The present study of their elastic properties throughout the structural phase transition of the Fe and Ce layers should be particularly relevant for the more general problem of understanding the crystal-to-glass transition in metallic materials, which is a matter of current debate. Experiments have revealed that this transformation is driven by a shear instability of the crystal lattice.^{11,12} An early calculation in a tight-binding model has predicted a reduction of the shear modulus in the glassy state by 20-40%.¹³

The presence of hydrogen during the growth process of the films results in a superstructure of alternating CeH_{1.2} and Fe layers, with different structural and magnetic properties.^{7,10,14} In particular, growth of the amorphous structure of the constituent layers is reduced to a thickness of 10 Å in both cases, and the Fe films can be deposited with a different texture if the substrate temperature is suitably chosen. In the present study we have probed the influence of these modifications on the elastic properties of the multilayers.

II. EXPERIMENTAL PROCEDURES AND SAMPLE STRUCTURE

The multilayer films were prepared by alternate sputtering of 99.9% pure cerium and 99.998% pure iron in an ultrahigh-vacuum (UHV) recipient (base pressure $\leq 5 \times 10^{-10}$ mbar) using an Ar-ion beam. Partial pressures of residual gases (e.g., O₂, N₂, H₂O) were below 10^{-10} mbar during deposition. Hydrided multilayers

CeH_x/Fe were grown by reactive sputtering in a hydrogen atmosphere of 8×10^{-6} mbar. Only cerium absorbs hydrogen, due to a large negative mixing enthalpy. Analysis by the (p, γ) resonant nuclear reaction of ^{15}N with hydrogen showed that the hydride composition is close to CeH_2 .¹⁵ Microscopy glass plates coated with a 100-Å-thick Cr buffer layer, with dimensions suitable for the vibrating-reed experiments (see below), were used as substrates. Deposition rates typically varied from 0.2 to 0.8 Å/s. Film thicknesses were designed by a computer-controlled quartz rate monitor, the bilayer wavelengths were varied between 24 and 200 Å, and the total film thickness of the multilayers always amounts to 5000 Å. To prevent oxidation on exposure to atmosphere, the multilayers were finally covered with a 60-Å-thick Cr layer.

The structure of the multilayer films has been well characterized previously by *in situ* reflection high-energy electron diffraction (RHEED) and x-ray diffraction at small and wide scattering angles in Θ - 2Θ Bragg-Brentano geometry, where the scattering vector is parallel to the film normal.⁷ The Ce/Fe multilayers were deposited at 90 K to minimize interfacial diffusion. The structure of the individual layers depends on their thicknesses. Up to critical values of about 20 Å for Fe and 60 Å for Ce the films grow in an amorphous structure. Above these thicknesses, crystalline Fe with bcc structure and preferred (110) orientation and crystalline fcc Ce with (111) texture are observed. There is no indication of the formation of the intermetallic compounds CeFe_2 and $\text{Ce}_2\text{Fe}_{17}$ allowed by the equilibrium phase diagram, for any of the multilayers. The structural coherence length in the crystalline layers parallel to their growth direction, as determined from the linewidths of the Bragg peaks using the Scherrer formula, corresponds to the thickness of the individual layers. This limit is not surprising in view of the large atomic-size mismatch between Fe and Ce (26% for the α -Ce phase; see below). The bcc Fe lattice perpendicular to the film plane is expanded by an average value of nearly 1%. As the critical thickness for the appearance of the amorphous phase is approached, this value increases somewhat and reaches about 3% at the disorder transition. But due to the partial superposition of the Fe layer (110) line, which is broadened because of the small perpendicular coherence length, and the broad intensity of the reflection from the amorphous Ce layers these values can only be estimated.

The hydrided multilayers $\text{CeH}_{\sim 2}/\text{Fe}$ were deposited at 90 K and also at room temperature. In contrast to the pure Ce/Fe system, amorphous growth of the individual $\text{CeH}_{\sim 2}$ and Fe layers in this heterostructure was observed up to a critical thickness value of 10 Å only. Above this value, the Fe layers (bcc structure) show a (110) texture for low-temperature and a (111) texture for room-temperature deposition, with an average lattice parameter enlarged by about 1.5% perpendicular to the film planes. $\text{CeH}_{\sim 2}$ (fcc structure) is always (111) textured. According to the RHEED diagrams there is a high degree of lateral order in the $\text{CeH}_{\sim 2}$ and Fe layers with (111) orientation, presumably due to the relatively small mismatch between the (111) surfaces (the Ce-Ce distance

is 3% smaller than twice the Fe-Fe distance). But since satellites near the (111) reflections in the x-ray diagrams are missing, there is no evidence for coherent $\text{CeH}_{\sim 2}$ -Fe interfaces.

An important problem to be addressed is that of the microscopic structure of the Ce-Fe and $\text{CeH}_{\sim 2}$ -Fe interfaces. The measured small-angle x-ray diffraction diagrams of the multilayers were modeled by Monte Carlo simulations invoking interfacial roughness and diffusion, as described in detail by Klose *et al.*⁷ It results that both systems maintain a well-defined layer structure with a sharp composition profile. Roughness may be quantified by a Gaussian fluctuation of the local layer thickness. In the Ce/Fe system the fluctuation full width at half maximum (FWHM) obtained is 1.2 atomic layers above the critical thickness where Fe is crystalline ($t_{\text{Fe}} > 20$ Å), and 1.3 atomic layers below where Fe is amorphous. Hydrogenation reduces the roughness of the interfaces: in the $\text{CeH}_{\sim 2}/\text{Fe}$ multilayers, local thickness fluctuations have a width of 1.0 atomic layers. Interdiffusion is negligible in both multilayer systems, except for low Fe layer thicknesses ($t_{\text{Fe}} \leq 20$ Å) where it is limited to the first atomic layer about the interface, amounting to 50% in Ce/Fe and to 20% in $\text{CeH}_{\sim 2}/\text{Fe}$. The extension of the interfaces defined by these values is corroborated by ^{57}Fe Mössbauer spectroscopy¹⁰ which, in particular, shows interfacial sharpening by hydrogenation.

The interaction of Ce and Fe at their common interface in the multilayers has a pronounced effect on the local electronic and magnetic structure near the interfacial zone. This clearly results from the ^{57}Fe Mössbauer spectra and from magnetic circular dichroism observed in x-ray absorption experiments.⁹ These experiments point to a strong hybridization between the Ce 5*d* and Fe 3*d* states in the Ce/Fe system. This is reflected by a "magnetic interface" which largely exceeds the extension of the structural interface. For details, the reader is referred to the preceding publications.^{9,10} For the elastic properties to be discussed here it is important that in the Ce/Fe multilayers Ce adopts, on a length scale of 15 Å at the interface, the electronic structure of the α phase with itinerant 4*f* states and a considerably reduced atomic volume as compared to the isostructural γ phase with localized 4*f* states (the difference is 17% in Ce metal). Evidently, this reduces the mismatch at the interfaces with Fe. Hence, for sufficiently large thicknesses, the Ce layers are composed of γ -phase-like Ce located in the center and α -phase-like Ce near the interfaces (we recall that Ce is amorphous up to a thickness of about 60 Å). Let us also mention that the α -like Ce atoms are magnetically polarized and carry an ordered magnetic 5*d* spin moment, in antiparallel orientation to the Fe 3*d* moment. In the hydrided multilayers $\text{CeH}_{\sim 2}/\text{Fe}$ a similar interfacial magnetic polarization is effective, but in this case the Ce atoms show a γ -like electronic configuration throughout the entire extension of the $\text{CeH}_{\sim 2}$ layer.¹⁶ Finally, we note that, since there is no experimental evidence for a structurally or electronically asymmetric interface in the multilayer systems, which *a priori* might be a distinct possibility, we assume that the interfaces are symmetric.

The elastic properties of the multilayer films were mea-

sured on flexural vibrations at room temperature using a vibrating-reed method. The modulus of elasticity determined is the flexural modulus. In the method applied, the resonance frequency of a bare metallized glass substrate is compared with the resonance of the same substrate coated with a multilayer on both sides to eliminate bending of the reed under the influence of static film stress. The flexural modulus of the film, E_F , is deduced from the frequency shift of the resonances:¹⁷

$$\frac{f_{S+F}^2}{f_S^2} = 1 + \left[3 \frac{E_F}{E_S} - \frac{\rho_F}{\rho_S} \right] \frac{t_F}{t_S}, \quad (1)$$

where f_{S+F} and f_S are the resonance frequencies of the reed carrying the multilayer and of the bare metallized substrate, respectively; t_F and t_S are the thicknesses of the multilayer and the substrate, ρ_F is the averaged effective density of the two multilayer components, and ρ_S and E_S the density and the flexural modulus of the substrate material, respectively.

The glass plate substrates, 110 or 145 μm thick, with lateral dimensions of 11.5 \times 8 mm², were precoated on both faces with a 100-Å-thick Cr layer by sputtering. Subsequently, they were mounted horizontally in a "cantilever beam" configuration, i.e., as a vibrating reed tightly clamped in a mounting holder at one end. The free end of the reed is driven by electrostatic excitation, and the vibration amplitude is detected in a capacitive way. The flexural moduli of the substrates E_S are given by the resonance frequencies of the cantilever modes:

$$f_n = \alpha_n (2n + 1)^2 \frac{\pi}{16\sqrt{3}} \frac{t_S}{l^2} \left(\frac{E_S}{\rho_S} \right)^{1/2}, \quad (2)$$

where α_n is a constant of the respective flexural mode, and l the length of the reed. All measurements were performed at the first flexural mode ($\alpha_0 = 1.425$), so resonances were obtained in the range between 700 and 800 Hz, with substrate moduli from 45 to 55 GPa. It is essential to point out that the entire holder with the mounted substrate can be removed from the vibrating-reed apparatus and then inserted into the UHV system for multilayer deposition. This provides the same clamping condition for the cantilever before and after deposition of the multilayers.

It is a general practice to compare the measured elastic moduli of layered composite systems like the ones of present concern to the moduli calculated using continuum elasticity theory. For a well-textured layer structure, like our samples in the case where the component layers Ce, CeH₂, and Fe are crystalline, we have a uniaxial symmetry: the crystallites exhibit a common orientation normal to the film but are randomly oriented in the plane of the film. In the reference system of the multilayer with the z axis along the growth direction this corresponds to a hexagonal symmetry, and the tensor of the effective elastic stiffness moduli has the nonvanishing components $C_{11} = C_{22}, C_{12}, C_{13} = C_{23}, C_{33}, C_{44} = C_{55}$, and $C_{66} = (C_{11} - C_{12})/2$; the flexural modulus is given by¹⁸

$$E_F = C_{11} - C_{13}^2 / C_{33}. \quad (3)$$

The elastic constants C_{ij} of the multilayer may be calculated from the primary elastic stiffness moduli of the bulk constituent layer material, c_{ij} , taken from the literature by using the expressions given by Grimsditch¹⁹ for the case of cubic crystal symmetry of the individual layers.

III. RESULTS AND DISCUSSION

A. Ce/Fe multilayers

The elastic properties of the Ce/Fe multilayers were measured on a series of films with different modulation wavelengths Λ , but equal thicknesses of the individual layers, $t_{\text{Ce}} = t_{\text{Fe}} = \Lambda/2$. The variation of the flexural modulus of the multilayer films with this value is presented in Fig. 1 in the relative form $\Delta E/E_S = (E_F - E_S)/E_S$ which by its sign reflects stiffening (> 0) or softening (< 0) of the reed. Below 30 Å, E_F decreases monotonically with decreasing sublayer thickness, indicating a strong softening of the reeds. The structural transition in the Fe layers into the amorphous phase is reflected by a pronounced minimum in $\Delta E/E_S$ ($\sim -50\%$) at 18 Å. Note that, according to the x-ray and RHEED diagrams, the Fe layers are clearly amorphous at this thickness and they are crystalline at the next larger thickness investigated here, $t_{\text{Fe}} = 22$ Å. On reducing the individual layer thickness further to 15 Å, $\Delta E/E_S$ rises steeply to the values adopted for thick crystalline Fe layers. Since the Ce sublayers are amorphous throughout the thickness range where the elastic anomaly occurs, it can be concluded that this anomaly essentially reflects the mechanical properties of the Fe layers. At the transition in the Ce layers from the amorphous to the crystalline fcc structure occurring near 60 Å, any anomaly in the relative variation of the flexural modulus of the multilayers, if it exists, must be within the error bars; obviously it must be much smaller than at the structural transition within the Fe layers.

To make a comparison of the measured flexural moduli of the Ce/Fe multilayers, E_F , with the results from the

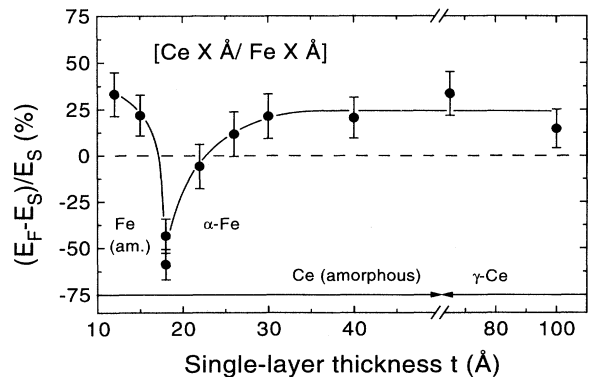


FIG. 1. Relative change of the flexural modulus $(E_F - E_S)/E_S$ at 300 K versus single-layer thickness of Ce/Fe multilayers ($t_{\text{Ce}} = t_{\text{Fe}} = \Lambda/2$, total thickness 5000 Å) deposited onto Cr-coated glass substrates (flexural modulus E_S) at 90 K. The solid line is a guide to the eye.

continuum theory of elasticity, we calculated E_F according to Eq. (3) from the film geometrical elastic constants C_{ij} in the way indicated above, using the listed values of the primary (crystallographic) moduli c_{ij} (i.e., c_{11} , c_{12} , and c_{44}) of bcc α -Fe and fcc γ -Ce (neglecting the presence of α -Ce at the interfaces⁹). It results that even for the largest periodicity length experimentally investigated ($\Lambda/2 = t_{Fe} = t_{Ce} = 100$ Å) the estimate of E_F is about a factor of 3 larger than the measured value. (If the α -like modification of Ce at the interfaces is taken into account this result will not be significantly modified.) The discrepancy may have several reasons which remain to be clarified. For example, (i) continuum elasticity theory may not be applicable for these heterostructures; (ii) the real structures of the individual Fe and Ce layers may be too far from those of the bulk crystals. But even though the low absolute value of the flexural modulus E_F deserves special attention, the most interesting feature in Fig. 1 is its remarkable relative variation with Λ which mainly reflects the variation with t_{Fe} .

An explanation of this variation must comprise the following points: (i) the elastic softening of the multilayers prior to the transition into the amorphous structure of the Fe layers, (ii) the low flexural modulus at the transition itself, and (iii) the elastic hardening in the amorphous phase with decreasing modulation length Λ . To date, no comprehensive theory exists that describes the relationship between a structural phase transition, as it is observed here, and elastic anomalies in metallic multilayers. In the following we therefore discuss the experimental data in Fig. 1 with reference to the mechanical properties (i) of multilayer systems investigated experimentally which show a transition from an amorphous into a crystalline structure, and (ii) of bulk alloy systems or intermetallic compounds that undergo a crystal-to-glass transition. Relevant theoretical models will briefly be addressed.

The physical mechanisms which are at the origin of the instability in the elastic response of the Ce/Fe system (Fig. 1) must be intimately related to the effects responsible for the amorphous growth of the Fe layers for sufficiently low thicknesses. Growth in an amorphous phase below a critical thickness has been observed for a number of layered thin-film heterostructures. This has been carefully investigated recently, for example, for Gd/Fe and Y/Fe sandwich structures by ^{57}Fe conversion-electron Mössbauer spectroscopy.^{20,21} The critical thickness for the change in the Fe layer growth mode is found to be 23 Å for both systems, which is very close to the value observed for the Ce/Fe multilayers. The authors attribute amorphous growth of the Fe layers on the Gd or Y sublayers (and vice versa) to an interfacial interaction effect which enforces the metastable structure. This interface effect is suggested to originate in the large mismatch between the Fe and Gd or Y layer lattice parameters, but a fundamental understanding of how this affects the growth mode is lacking. Presumably, amorphous growth of Fe on a rare-earth sublayer (or of a rare earth on an Fe layer) is favored when this one is amorphous itself. According to the similar chemical and structural properties of the rare earths, the mechanisms

should be the same for all combinations of these elements with Fe. The experiments on Gd/Fe and Y/Fe thin-film structures have revealed that, when the Fe layer thickness surpasses the critical thickness, a transformation of the amorphous phase into a polycrystalline bcc structure throughout the entire Fe layer occurs. According to previous structural and magnetic investigations,^{7,8} the Ce/Fe system shows the same behavior, i.e., the amorphous Fe phase is not present at the interface above the critical thickness.

Recently, the elastic properties of other lattice-mismatched multilayers, W/Ni (Ref. 6) and Ag/Ni (Ref. 22) deposited by sputter deposition, were reported. These systems show a similar disorder transition from a crystalline to an amorphous structure with decreasing modulation length Λ . Elasticity was probed by Brillouin light scattering experiments which were used to measure, via the phase velocity of a suitable acoustic mode, the elastic constant C_{44} and, in the case of the Ag/Ni system, also C_{11} and C_{33} . For both systems the shear modulus C_{44} decreases by about 40% with decreasing Λ , over an extended length scale down to the disorder transition at $\Lambda \approx 30$ Å (W/Ni) and ≈ 20 Å (Ag/Ni), respectively, where both composite materials in the two systems become amorphous. In the amorphous phase, C_{44} is nearly Λ independent (W/Ni) or increases abruptly (Ag/Ni). For Ag/Ni, C_{33} decreases monotonically with decreasing Λ through the disorder transition, while C_{11} does not vary substantially in the entire Λ range covered. X-ray diffraction experiments reveal that in both multilayer systems the elastic anomaly is accompanied by a lattice distortion. This distortion increases with decreasing modulation length Λ , as a precursor of the structural transition. The structure of the W/Ni multilayers was investigated in great detail.⁶ The average lattice spacing along the film normal expands monotonically, reaching $\sim 2\%$ near the disorder transition. Modeling the multilayer shows that each material is strained anisotropically, in particular the Ni layers, so that the lattice symmetry is no longer cubic.

These experiments provide convincing evidence that the elastic anomalies of metallic multilayer systems are correlated with structural anomalies, but do not reveal the underlying mechanism. In their discussion of the W/Ni system, the authors propose two likely origins for the anomalous softening of the elastic response: (i) decreased bonding of the atomic layers with increased lattice expansion, and (ii) disorder at the incoherent interfaces. We hypothesize that these mechanisms may also apply for the Ce/Fe system for thicknesses t_{Fe} above the disorder transition in the Fe layers and that the origin of the elastic softening is the same, even though the observed expansion of the Fe layer lattice spacing remains to be quantified with higher precision and even though different elastic moduli were probed for the different systems. In particular, the flexural response of a multilayer, as studied here for the Ce/Fe system, involves an interplay between the elastic constants C_{11} , C_{13} , and C_{33} [Eq. (3)], which cannot be separately determined by a simple measurement of E_F . Hence the behavior of any single modulus C_{ij} with respect to the lattice softening and the

subsequent mechanical instability cannot be isolated. On the other hand, the shear elastic constant C_{44} of the W/Ni system is derived from the velocity of the surface acoustic wave which only weakly depends on C_{11} , C_{13} , and C_{33} . Nevertheless, it may safely be assumed that, as suggested for W/Ni, interfacial disorder plays an important role for the elastic anomaly in the Ce/Fe multilayers, too. As the modulation length Λ and hence $t_{\text{Fe}} = t_{\text{Ce}}$ is decreased towards the structural transition in the Fe layers, an increasing volume fraction of the material is affected by the structural disorder introduced by the large mismatch of the interatomic spacings at the interface of the bcc Fe and amorphous Ce layers. This is accompanied by a drastic decrease of E_F (Fig. 1). At a critical defect concentration the system undergoes a crystalline-to-amorphous transition.

A number of theoretical studies have attempted to attribute the elastic anomalies in a multilayered metallic material to the lattice expansions observed. Support comes, for example, from experiments on Ag/Co superlattices,²³ showing that irradiation with high-energy ions simultaneously reduces the anomalous shear modulus softening and lattice expansion. The model calculations differ in the origin of this expansion; they are based on either structural or electronic arguments. It is beyond the scope of this paper to discuss them here. Structural models have attributed the lattice expansions to stress at the interfaces. Such interface stresses are predicted to be substantially larger at incoherent than at coherent interfaces, and to induce large elastic strains as a function of the periodicity length Λ .⁴ It has been shown³ that electron-transfer effects can contribute to strain in metallic multilayers. As we have mentioned above, interfacial electronic interaction plays an important role in the Ce/Fe system: it leads to a strong hybridization of the Fe 3d and Ce 5d states. As a consequence, an increasing amount of Ce near the interface adopts the α -phase electronic configuration with delocalized 4f states as Λ is decreased.⁹ In the α phase, Ce has a 17% smaller atomic volume. Hence the variation with Λ , i.e., with t_{Ce} , in the fraction of the γ - and α -phase-like parts in the Ce layers certainly will produce Λ -dependent strain and thus will have a bearing on the elastic properties.

Wolf and co-workers²⁴⁻²⁶ have used molecular dynamics to show that the elastic anomalies of lattice-mismatched multilayers originate in a combined effect of the structural disorder due to—and localized at—the interfaces and of lattice expansion. The calculations were performed for a superlattice, where thin layers of the same fcc material are periodically rotated with respect to each other about the film normal to introduce interfacial disorder by the formation of grain boundaries. Hence chemical effects are excluded. The authors find that for an incoherent interface the structural disorder near the grain boundary gives rise to a volume expansion, mostly directed along the layer normal, concentrated near the interface, and proportional to the amount of disorder. Disorder gains in importance with decreasing modulation length Λ . The result is a decreased elastic constant C_{44} (which probes shear strain parallel to the layer plane). For C_{33} (characterizing the effect of strain perpendicular

to the plane), volume expansion softens and structural disorder hardens, and hence they oppose each other. For small Λ , mutual interaction of neighboring grain-boundary interfaces (via overlapping elastic strain fields) may lead to extremal values of some elastic moduli. These calculations are in qualitative agreement with the observations on a number of multilayer systems (see, for example, Ref. 5). But it is clear that the underlying simple model system is far from the Ce/Fe system. Hence only the general theoretical findings, i.e., the close correlation between the elastic anomalies and the interfacial disorder, together with the concomitant volume expansion, may qualitatively apply. Let us point out that the observed softening of the flexural modulus E_F in Ce/Fe with decreasing Λ cannot be attributed to the grain boundaries within the polycrystalline Fe layers, since the grain size does not vary significantly with their thickness t_{Fe} .⁷

The anomaly appearing in the flexural modulus E_F of the Ce/Fe multilayers when passing through the disorder transition in the Fe sublayers must be closely related to the elasticity anomaly observed around the crystal-to-glass transition in intermetallic compounds and alloys. Such a transformation occurs, for example, in the compound Zr_3Al under heavy-ion irradiation.²⁷ With increasing fluence, the averaged shear-wave velocity is found to decrease continuously in the progressively disordered crystal, together with an increasing volume dilatation. At a critical dose, the material undergoes a transition to a glassy state. Here, the shear-wave velocity has dropped by $\sim 50\%$; it increases slightly under further irradiation. In a recent investigation of mechanically alloyed $\text{Zr}_{1-x}\text{Al}_x$, Ettl and Samwer¹² found a drastic decrease of the isotropic shear modulus (determined from the Debye temperature via specific-heat measurements) with increasing Al content x , and finally (at $x = 0.2$) a structural transformation into an amorphous phase. As x is further increased, the shear modulus gradually recovers to almost its value adopted near $x = 0$. It is important to note that in both materials substantial elastic softening precedes amorphization as a precursor to a mechanical instability. Obviously, this is very similar to what is observed in the Ce/Fe multilayers. This may imply that the origin of the softening is the same.

Li and Johnson²⁸ applied molecular dynamics to a fcc binary random solid solution with varying atomic-size ratios and concentrations to simulate the crystal-to-glass transition. It occurs at a critical supersaturated solute concentration below a critical solute-solvent atomic-size ratio of 0.85, in qualitative agreement with an earlier argument of Egami and Waseda.²⁹ Just prior to the amorphization, the shear elastic moduli $c' = (c_{11} - c_{12})/2$ and c_{44} related to tetragonal and rhombohedral lattice distortions, respectively, decrease dramatically with increasing solute concentration, together with a martensite-like structural change; in the amorphous region, c' increases again (here, the c_{ij} are given in the crystallographic reference system). These results were experimentally confirmed by the elastic behavior of the $\text{Zr}_{1-x}\text{Al}_x$ alloys,¹² which we have described above. The authors conclude that softening of the shear elastic responses plays a crucial role for the stability of the crystalline

phase. The transition to the amorphous phase seems to be correlated to a mechanical instability occurring for a small elastic stiffness.

In the metastable binary solid solutions the atomic-size mismatch leads to random local stress fields. These can be similarly created by radiation damage. Kulp *et al.*³⁰ studied radiation-damage induced amorphization by a molecular dynamics simulation. The authors conclude that atomic-level shear stresses provide a universal criterion for the attainment of the amorphous state; they have to reach a critical value for the transition to occur, irrespective of the particular amorphization process. Li and Johnson suggest²⁸ that the effect of the local random shear stress fields is to frustrate the local shear deformations within the crystalline lattice and thus result in a transition to a structural glass, in much the same manner as random magnetic fields frustrate local spin orientations in magnetic systems and, if sufficiently strong, lead to the formation of a spin glass.³¹

The Ce/Fe multilayers are a remarkable example of a system where a structural and magnetic disorder transition occur simultaneously. The variations of the flexural modulus E_F of the layered system (Fig. 1) and of the (tetragonal) shear modulus $(c_{11} - c_{12})/2$ of the metastable binary alloys through the crystalline-to-amorphous transition show striking similarities. This suggests that the mechanisms underlying the elastic anomaly in the bulk alloys may be similarly effective in the layered composite structure. But we must await theoretical work dealing with the crystalline-to-amorphous transition in such systems before this hypothesis can be confirmed or must be disproved. Figure 2 shows that the structural transition in the Fe layers of the Ce/Fe system is accompanied by a steep drop of the spontaneous magnetization and an appreciable increase of the low-temperature coercive field;³² the Curie temperature is reduced to values below 180 K.⁸ In the amorphous phase the magnetic structure is not collinear and, according to low-field magnetic susceptibility results,³³ it is possible that magnetic order is induced by the external magnetic field applied for the measurements. Yu and Kakehashi³⁴ have predicted a spin-glass ground state for amorphous Fe; they attribute ferromagnetism recently observed²¹ in Y/Fe layered structures to a volume effect, i.e., to an increase of the Fe-Fe distance caused by the Y atoms at the interface.

B. CeH_{~2}/Fe multilayers

The elastic properties of CeH_{~2}/Fe multilayers were measured on a series of films with either a (110) or a (111) texture of the individual Fe layers. Figure 3 shows the relative change of the flexural modulus of the multilayer films E_F with varying Fe layer thickness of 16, 30, and 50 Å. The thickness of the CeH_{~2} layers was kept constant at 16 Å. Let us recall that the individual layers are crystalline in these structures.⁷ Obviously, hydrogenation causes a profound change in the mechanical properties of the multilayers. It may be noted that (i) the flexural moduli of the hydrided multilayers are substantially enhanced compared to the values displayed in Fig. 1; (ii) a difference on the order of ~50% in the relative value

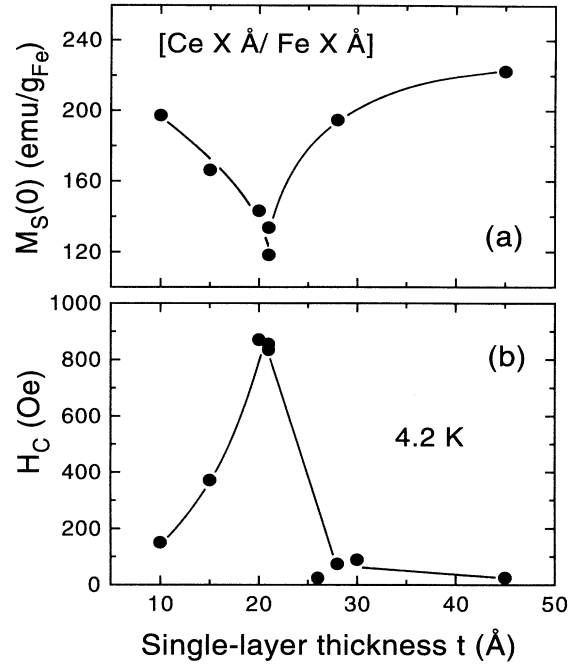


FIG. 2. (a) Spontaneous magnetization $M_S(0)$ and (b) coercive field H_C at 4.2 K versus single-layer thickness ($t_{Ce} = t_{Fe} = \Lambda/2$) of Ce/Fe multilayers with 2000 Å total film thickness, deposited onto Cr-coated Si(100) (Ref. 32). Solid lines are guides to the eye.

$\Delta E/E_S$ is found for the multilayers with the differently textured Fe layers at a given thickness.

The difference in the flexural moduli for the two Fe textures observed may be explained to a large part by the results of Baral *et al.*,¹⁸ who calculated the flexural modulus E_F of a thin foil with a (110) and (111) texture in terms of the primary elastic constants c_{ij} . For the (110) texture the expression is

$$E_F = \frac{9c_{11} + 7c_{12} + 14c_{44}}{16} - \frac{(c_{11} + 3c_{12} - 2c_{44})^2}{8(c_{11} + c_{12} + 2c_{44})}, \quad (4)$$

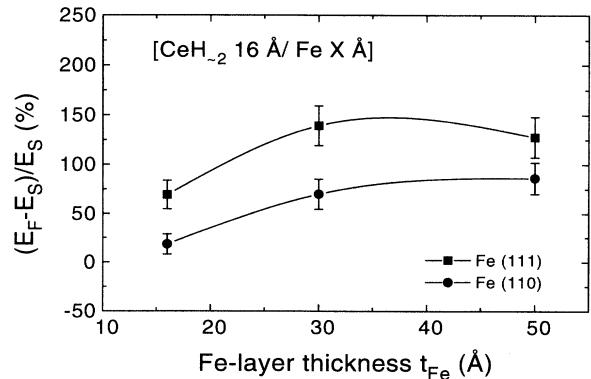


FIG. 3. Relative change of the flexural modulus $(E_F - E_S)/E_S$ of CeH_{~2}/Fe multilayers (total thickness 5000 Å) at 300 K with variation of the Fe layer thickness for (111) and (110) texture (solid lines: guide to the eye). Cr-coated glass substrates with flexural modulus E_S .

and for the (111) texture

$$E_F = \frac{c_{11} + c_{12} + 2c_{44}}{2} - \frac{(c_{11} + 2c_{12} - 2c_{44})^2}{3(c_{11} + 2c_{12} + 4c_{44})}. \quad (5)$$

With the elastic constants of bulk Fe (Ref. 35) this yields the flexural moduli of 257.3 GPa for the (110) texture and 275.1 GPa for the (111) texture, respectively. When referred to an averaged substrate modulus $E_S = 50$ GPa, these numbers result in a $\sim 40\%$ higher $\Delta E/E_S$ value for a Fe (111) texture with respect to a (110) texture. This shows that the difference in the flexural moduli of the CeH_{~2}/Fe multilayers with the two textures mainly reflects a property of the Fe sublayers. However, a contribution of the interfaces with the CeH_{~2} layers cannot be excluded. Wolf²⁶ has shown in the grain-boundary model of a metallic superlattice that the grain-boundary energy, which is a direct measure of the amount of structural disorder in the system, depends sensitively on the crystallographic orientation of the planes involved in forming the interface; as a consequence, the elastic response is different. In the CeH_{~2}/Fe system the mismatch and hence disorder at the interface is smaller for the (111) texture of the Fe layers, and according to Fig. 3 this is connected with a harder material. According to Eq. (3) the flexural modulus E_F reflects a complex interplay between the effective elastic constants C_{11} , C_{13} , and C_{33} , which may be softened (C_{11} , C_{13}) or, counter to intuition, strengthened (C_{33}) by the structural disorder at the interfaces.²⁶ Apparently, the softening effect in C_{11} dominates the elastic response of the CeH_{~2}/Fe multilayers. Let us finally point out that the volume contribution of the hydrided Ce sublayers to the flexural modulus of the multilayers is not clear. In this context it would be of particular interest to study the influence of a variation in the hydrogen content of the system.

IV. CONCLUSION

A vibrating-reed technique has been used to measure the mechanical properties of multilayers composed of Ce and Fe. The structural transition from an amorphous to the bcc crystalline phase occurring in the Fe sublayers at a critical thickness near 20 Å is reflected in a drastic decrease (of $\sim 70\%$) of the flexural modulus. The elastic softening is observed already for crystalline Fe sublayers above the critical thickness for amorphous growth, and hence is a precursor effect rather than the consequence of amorphization. This reveals conspicuous similarities to the crystal-to-glass transition in bulk metallic materials, which seems to be driven by a shear instability of the crystal lattice.

In hydrided multilayer structures CeH_{~2}/Fe the Fe sublayers grow in the bcc structure above 10 Å, with a pronounced (110) or (111) texture for low- or room-temperature deposition, respectively. The differences in the flexural moduli of the multilayers observed for the two Fe textures result to a large extent from the bulk properties of the Fe layers, even though interfacial effects cannot be excluded. For these multilayers it will be interesting to extend the measurements to low temperatures, where a reorientation transition of the magnetic easy axis from in plane to out of plane has been observed recently.¹⁰ These measurements are in progress.

ACKNOWLEDGMENTS

We would like to thank O. Schulte and F. Klose for useful discussions, and K. Samwer for helpful correspondence. This work was supported by the Deutsche Forschungsgemeinschaft within SFB 345. In addition the grant-in-aid to one of the authors (R.H.) by the Graduiertenförderung des Landes Niedersachsen is gratefully acknowledged.

¹For a recent review, see, for example, I. K. Schuller, A. Far-tash, and M. Grimsditch, *Mater. Res. Soc. Bull.* **15**, 33 (1990).

²T. B. Wu, *J. Appl. Phys.* **53**, 5265 (1982); W. E. Pickett, *J. Phys. F* **12**, 2195 (1982); R. C. Cammarata, *Scr. Metall.* **20**, 479 (1986).

³M. L. Huberman and M. Grimsditch, *Phys. Rev. Lett.* **62**, 1403 (1989); *Phys. Rev. B* **46**, 7949 (1992).

⁴See, for example, F. H. Streitz, R. C. Cammarata, and K. Sieradzki, *Phys. Rev. B* **49**, 10707 (1994).

⁵E. E. Fullerton, I. K. Schuller, F. T. Parker, K. A. Svinarich, G. L. Eesley, R. Bhadra, and M. Grimsditch, *J. Appl. Phys.* **73**, 7370 (1993).

⁶E. E. Fullerton, S. Kumar, M. Grimsditch, D. M. Kelly, and I. K. Schuller, *Phys. Rev. B* **48**, 2560 (1993).

⁷F. Klose, M. Steins, T. Kacsich, and W. Felsch, *J. Appl. Phys.* **74**, 1040 (1993).

⁸J. Thiele, F. Klose, A. Schurian, O. Schulte, W. Felsch, and O. Bremert, *J. Magn. Magn. Mater.* **119**, 141 (1993).

⁹F. Klose, O. Schulte, F. Rose, W. Felsch, S. Pizzini, C. Giorgetti, F. Baudelet, E. Dartyge, G. Krill, and A. Fontaine, *Phys. Rev. B* **50**, 6174 (1994).

¹⁰Ph. Bauer, F. Klose, O. Schulte, and W. Felsch, *J. Magn. Magn. Mater.* **138**, 163 (1994).

¹¹W. L. Johnson, M. Li, and C. E. Krill III, *J. Non-Cryst. Solids* **156–158**, 481 (1993).

¹²C. Ettl and K. Samwer, *Mater. Sci. Eng. A* **178**, 245 (1994).

¹³F. Cyrot-Lackmann, *Phys. Rev. B* **22**, 2744 (1980).

¹⁴F. Klose, J. Thiele, A. Schurian, O. Schulte, M. Steins, O. Bremert, and W. Felsch, *Z. Phys. B* **90**, 79 (1993).

¹⁵A. Weidinger and F. Klose (unpublished).

¹⁶O. Schulte, F. Baudelet, F. Manar, C. Giorgetti, E. Dartyge, G. Krill, and W. Felsch (unpublished).

¹⁷B. S. Berry and W. C. Pritchett, *IBM J. Res. Dev.* **19**, 334 (1975).

¹⁸D. Baral, J. E. Hilliard, J. B. Ketterson, and K. Miyano, *J. Appl. Phys.* **53**, 3552 (1982).

¹⁹M. H. Grimsditch, *Phys. Rev. B* **31**, 6818 (1985).

²⁰J. Landes, Ch. Sauer, B. Kabius, and W. Zinn, *Phys. Rev. B* **44**, 8342 (1991).

²¹S. Handschuh, J. Landes, U. Köbler, Ch. Sauer, G. Kisters, A. Fuss, and W. Zinn, *J. Magn. Magn. Mater.* **119**, 254 (1993).

²²G. Carlotti, D. Fioretto, G. Socino, B. Rodmacq, and V. Pelo-

- sin, *J. Appl. Phys.* **71**, 4897 (1992).
- ²³E. E. Fullerton, I. K. Schuller, R. Bhadra, M. Grimsditch, and S. M. Hues, *Mater. Sci. Eng. A* **126**, 19 (1990).
- ²⁴D. Wolf and J. F. Lutsko, *Phys. Rev. Lett.* **60**, 1170 (1988).
- ²⁵S. R. Phillpot, D. Wolf, and S. Yip, *Mater. Res. Soc. Bull.* **15**, 38 (1990).
- ²⁶D. Wolf, *Mater. Sci. Eng. A* **126**, 1 (1990).
- ²⁷P. R. Okamoto, L. E. Rehn, J. Pearson, R. Bhadra, and M. Grimsditch, *J. Less-Common Met.* **140**, 231 (1988).
- ²⁸M. Li and W. L. Johnson, *Phys. Rev. Lett.* **70**, 1120 (1993).
- ²⁹T. Egami and Y. Waseda, *J. Non-Cryst. Solids* **64**, 113 (1984).
- ³⁰D. T. Kulp, T. Egami, D. E. Luzzi, and V. Vitek, *J. Non-Cryst. Solids* **156-158**, 510 (1993).
- ³¹K. Binder and A. P. Young, *Rev. Mod. Phys.* **58**, 801 (1986).
- ³²J. Thiele, F. Klose, O. Schulte, A. Schurian, and W. Felsch, *Appl. Surf. Sci.* **65/66**, 175 (1993).
- ³³O. Schulte and W. Felsch (unpublished).
- ³⁴M. Yu and Y. Kakehashi, *Phys. Rev. B* **49**, 15 723 (1994).
- ³⁵*Smithells Metals Reference Book*, edited by E. A. Brandes (Butterworth, London, 1983); *Landolt-Börnstein New Series*, edited by K. H. Hellwege and A. M. Hellwege, Group III, Vols. 11 and 18 (Springer, Berlin, 1979 and 1984).